PCCP

Structural Characterization of Molybdenum-Dinitrogen Complex as Key Intermediate toward Ammonia Formation by Dispersive XAFS Spectroscopy

Journal:	*Physical Chemistry Chemical Physics*
Manuscript ID	CP-COM-12-2019-006761.R4
Article Type:	Communication
Date Submitted by the Author:	21-Apr-2020
Complete List of Authors:	Yamamoto, Akira; Kyoto University, Graduate School of Human and Environmental Studies Arashiba, Kazuya; The University of Tokyo, School of Engineering, Naniwa, Shimpei; Kyoto University, Graduate School of Human and Environmental Studies Kato, Kazuo; Japan Synchrotron Radiation Research Institute, Tanaka, Hiromasa; Daido University, School of Liberal Arts and Sciences Yoshizawa, Kazunari; Kyushu University, Institute for Materials Chemistry and Engineering Nishibayashi, Yoshiaki; The University of Tokyo, School of Engineering, Yoshida, Hisao; Kyoto University, Graduate School of Human and Environmental Studies

COMMUNICATION

Structural Characterization of Molybdenum-Dinitrogen Complex as Key Species toward Ammonia Formation by Dispersive XAFS Spectroscopy

Received 00th January 20xx,
Accepted 00th January 20xx

DOI: 10.1039/x0xx00000x

www.rsc.org/

Akira Yamamoto,[*a,b] Kazuya Arashiba,[c] Shimpei Naniwa,[a] Kazuo Kato,[d] Hiromasa Tanaka,[e] Kazunari Yoshizawa,[f] Yoshiaki Nishibayashi,[*c] and Hisao Yoshida[*a,b]

Structural characterization of a hardly-isolatable molybdenum-dinitrogen complex bearing a PNP-type pincer ligand, which is assumed to be a key reactive complex in stoichiometric transformation of molybdenum triiodide complex [MoI_3(PNP)] into the corresponding molybdenum nitride complex under an atmospheric pressure of dinitrogen, was carried out by dispersive XAFS.

In industry, ammonia is produced from dinitrogen and dihydrogen via the Haber–Bosch process using a heterogeneous catalyst under high temperature and pressure to obtain the sufficient reaction rate and conversion.[1] In sharp contrast to high temperature and pressure reaction conditions in heterogeneous reaction systems, in 2003 Schrock and Yandulov firstly reported the catalytic ammonia formation from dinitrogen with a reductant and a proton source in the presence of a catalytic amount of a molybdenum-dinitrogen complex bearing a tetradentate ligand under ambient reaction conditions, where 8 equiv. of ammonia were formed on the catalyst.[2] Since the first report, some research groups have reported the catalytic ammonia formation using transition metal–dinitrogen complexes as catalysts under mild reaction conditions to produce ammonia and/or hydrazine effectively.[3-7] Quite recently, our group has reported an extremely high efficient reaction system of direct conversion of dinitrogen into ammonia with samarium diiodide as a reductant and water as a proton sources in the presence of a catalytic amount of molybdenum trichloride complexes bearing pincer ligands, where the amount of ammonia formation reached to 4,350 equiv.[7m] based on the catalyst together with the high reaction rate of the ammonia formation. In this reaction system, cleavage of the nitrogen–nitrogen triple bond (N≡N) of dinitrogen readily proceeds under ambient reaction conditions despite its large bond dissociation energy of N≡N (945 kJ mol^{-1}). Based on results of DFT calculations on the reaction pathway, we proposed dinitrogen-bridged dimolybdenum complexes such as [MoI(**PNP**)]$_2$(μ-N_2) (**1**; **PNP** = 2,6-bis(di-*tert*-butylphosphinomethyl)pyridine) as key reactive intermediates for the scission of the bridging dinitrogen ligand in the Mo–N≡N–Mo core.[7i] However, unfortunately, we have not yet obtained experimental information on the molecular structure of the dinitrogen-bridged dimolybdenum complexes.

There are many well-known techniques to characterize molecular structures of reactive intermediates. Although X-ray crystal structure analysis provides direct information on molecular structures, isolation of key reactive intermediates as single crystals is necessary for the X-ray crystal structure analysis. In contrast, XAFS technique is a powerful tool to reveal the chemical state and local geometry of the target element even in homogeneous transition metal complexes.[8] The utilization of XAFS spectroscopy prompted us to investigate structural characterization of a hardly-isolatable molybdenum complex as a key reactive complex under catalytic reaction conditions.

Previously, we found that the reaction of [MoI_3(**PNP**)] (**2**) with 3 equiv. of decamethylcobaltocene ($CoCp^*_2$, Cp^* = η^5-C_5Me_5) as a reductant under an atmospheric pressure of nitrogen gas (N_2) at room temperature gave the corresponding nitride complex [Mo(≡N)I(**PNP**)] (**3**).[7i] In this reaction system, the formation of **3** is assumed to proceed via scission of the bridging dinitrogen in **1** as a key reactive intermediate (**Scheme 1**).[7i] Herein, we attempt to observe such an reactive Mo complex at low-temperature under an atmospheric pressure of N_2 by dispersive XAFS (DXAFS) spectroscopy.

[a] Department of Interdisciplinary Environment, Graduate School of Human and Environmental Studies, Kyoto University, Yoshida Nihonmatsu-cho, Sakyo-ku, Kyoto 606-8501, Japan
[b] Elements Strategy Initiative for Catalysts & Batteries (ESICB), Kyoto University, Kyotodaigaku Katsura, Nishikyo-ku, Kyoto 615-8520, Japan
[c] Department of Systems Innovation, School of Engineering, The University of Tokyo, Hongo, Bunkyo-ku, Tokyo 113-8656, Japan
[d] Japan Synchrotron Radiation Research Institute, SPring-8, Sayo, Hyogo 679-5198, Japan
[e] School of Liberal Arts and Sciences, Daido University, Minami-ku, Nagoya 457-8530, Japan
[f] Institute for Materials Chemistry and Engineering, Kyushu University, Nishi-ku, Fukuoka 819-0395, Japan

† Footnotes relating to the title and/or authors should appear here.
Electronic Supplementary Information (ESI) available: [details of any supplementary information available should be included here]. See DOI: 10.1039/x0xx00000x

Mo K-edge DXAFS spectra were measured at BL28B2 of SPring-8, (Hyogo, Japan). The temperature of the reactor was kept at 198 K using a cooling bath (dry-ice ethanol) as shown in **Scheme 1**. The XAFS data was analysed using the Athena and Artemis programs with the theoretical standards calculated using FEFF.[9] Detailed experimental procedures are shown in the Supplemental Information.

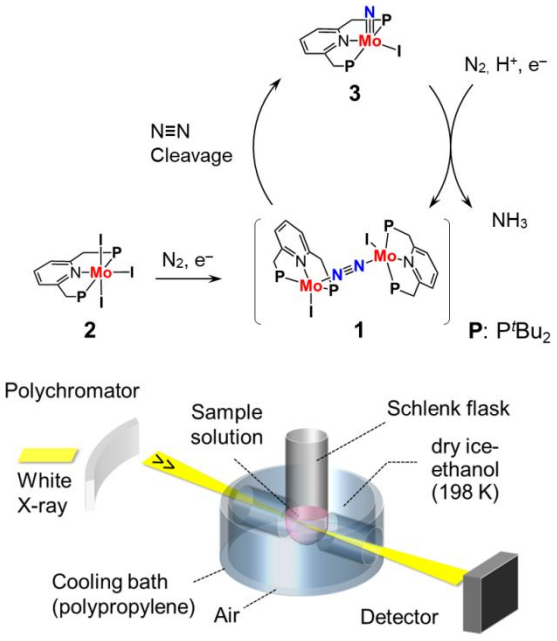

Scheme 1. A simplified proposed reaction mechanism of catalytic ammonia synthesis from dinitrogen by Mo complex at room temperature,[7i] and a schematic illustration of the experimental set-up in this study.

First, we started DXAFS measurements in the reduction process of **2** with 2 equiv. of $CoCp^*_2$ in tetrahydrofuran (THF) at room temperature (*i.e.*, without cooling) under an atmospheric pressure of N_2. As expected, **2** was rapidly converted into **3** within 10 min based on the change of XANES spectra. However, unfortunately, during the reduction process, a spectrum of any transient Mo complex was not observed at all. Next, we performed reduction of **2** at 198 K under an atmospheric pressure of N_2 using a cooling bath of dry-ice ethanol. Reduction process of **2** (20 µmol) in THF was monitored by the DXAFS measurement. Time profile of the XANES spectra after addition of $CoCp^*_2$ (2.0 equiv. based on **2**; 40 µmol) as a one-electron reductant is shown in **Fig. 1(a)**. The spectrum changed immediately after the addition of $CoCp^*_2$, and no further change was observed during 22 min (see **Fig. S1** in **ESI** for the detailed comparison). The normalized peak intensity at 20012 eV was also plotted with the reaction time (**Fig. 1(b)**), and did not change markedly at 198 K for 22 min. This result indicates that formed Mo species (referred to as **A**) is stable at this temperature. To check the stability of **A**, the DXAFS measurement was done again after removing the cooling bath up to room temperature and stirring at room temperature for further 4 min (after 60 min from the addition of $CoCp^*_2$). This operation largely changed the spectrum to the red one in **Fig. 1(a)**, and the shape of the reaction mixture was quite similar to that of **3** as shown in **Fig. S1**. Thus, the Mo species **A** observed at 198 K would be rapidly converted into **3** at room temperature.

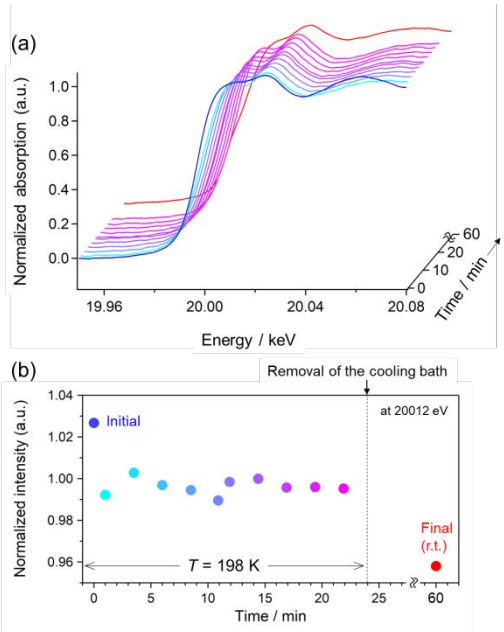

Fig. 1 (a): In situ XANES spectra of reduction process of **2** in THF before (blue) and after (light blue to pink) addition of $CoCp^*_2$ at 198 K, and after 60 min at 298 K (red). The detail comparison was shown in **Fig. S1**. (b): A time profile of normalized intensity at 20012 eV.

To obtain information on the coordination structure of **A**, we performed the XANES simulation using the FDMNES program[10] from the structure model of crystallographic data or optimized structure by DFT calculations (**ESI**). Before the comparison, we checked the effect of temperature on the XANES shape using **2** in THF (**Fig. S2**), and confirmed that the shape did not change at room temperature and 198 K. Then, to guarantee the validity of the simulation in our Mo samples, we performed the simulation using Mo foil, **2**, and **3**. In the Mo foil, the experimental XANES spectrum was successfully reproduced with the characteristic features (**Fig. S3**) although not an exact match. For the simulation of **A**, two dimolybdenum complexes with one I^- ion in a Mo centre were used with or without terminal N_2 ligands (**Fig. 2(b)**, **1** and $[MoI(N_2)(\mathbf{PNP})]_2(\mu\text{-}N_2)$ (**4**)).[11] Without the terminal N_2 ligands (**1**), a clear pre-edge peak was observed in the simulation; on the other hands, the peak was not observed with the terminal N_2 ligands (**4**). The pre-edge peak is assigned to the 1*s*–4d transition in the Mo K-edge XANES spectra,[12] and the intensity was affected by the local symmetry of the molybdenum atom. Typically, octahedral (*i.e.*, six coordination) complex with high symmetry shows low (or no) pre-edge peak, and the peak intensity increases with increasing the degree of distortion of the structure into pyramidal (*i.e.*, five coordination).[13] Thus, the simulation results indicate that the pre-edge feature provides the information of the local structure of the Mo complex. The experimental spectra of **A** did not show the pre-edge feature (**Fig. 2(a)**), which suggesting that **A** has six-coordination structure with a high symmetry. Besides, we performed the XANES simulation of the mononuclear six-coordination Mo complex ($[MoI(N_2)_2(\mathbf{PNP})]$, **5**), which show the

similar spectral feature with that of **4**. Based on these results, the most likely candidate for **A** would be **4** or **5** with a six-coordination structure, which can be converted to **1** by elimination of N_2 to according to **eq. 1**.

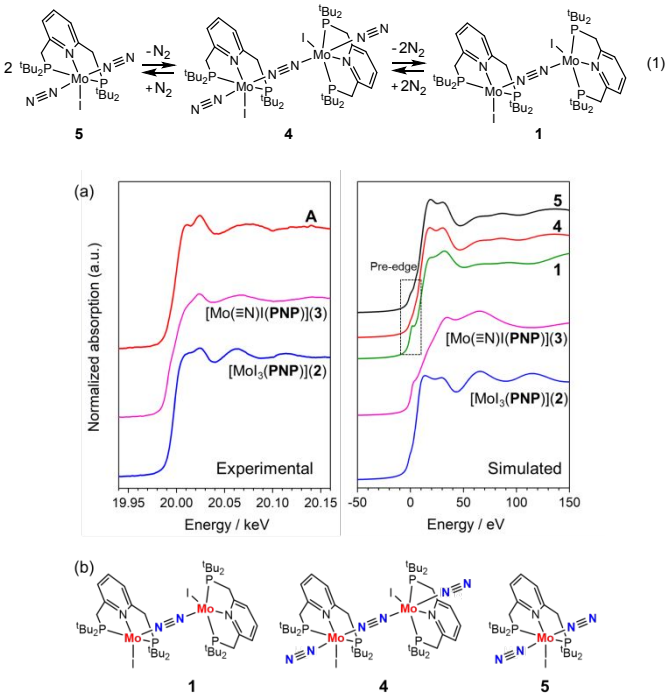

Fig. 2 (a) Comparison between experimental XANES spectra (left) and simulated XANES spectra by FDMNES (right). The reference spectra were obtained at room temperature using THF as a solvent. (b) Structures of **1**, **4**, and **5** used in the simulation.

To obtain the structural information of **A**, we analysed the EXAFS spectra obtained simultaneously at the experiment in **Fig. 1**. The Fourier-transformed EXAFS spectra after the addition of $CoCp^*_2$ (2.0 equiv.) into Mo complex **2** in THF is shown in **Fig. 3(a)**. The addiction of $CoCp^*_2$ immediately decreased the band intensity of Mo–I scattering around 2.58 Å,[14] and the spectra become stable up to 22 min (**Fig. 3(b)**), which was the same trend as the XANES data. The decrease of the band of Mo–I scattering indicates the I^- ions are removed from the Mo centre by the reduction process of **2**. The Mo–I band intensity after addition of $CoCp^*_2$ was lower than that of a newly prepared Mo(II) complex [MoI_2(**PNP**)] (**6**) (green line) and similar to **3** (red line) (**ESI**) as shown in **Fig. 3(b)**, which suggests that one I^- ion was coordinated to the Mo centre. On the other hand, the other band intensities at 1.5 and 2.0 Å did not change markedly. By the curve-fitting analysis using three shells of Mo–I, –P, and –N, the spectrum of **A** was successfully reproduced with the R factor of 1.4% (**Fig. 3(c), Table 1**), which also supports the proposed structure of **4 or 5**. Although, the scattering band of Mo–Mo in the Mo–(N≡N)–Mo core was not confirmed in this condition unfortunately,[15] the EXAFS analysis supports the existence of one Mo–I bond in **A** by the stoichiometric reduction of **2**.

In summary, a DXAFS spectroscopy was used for the structural characterization of a Mo complex as a key reactive species in the stoichiometric reduction process of [MoI_3(**PNP**)] (**2**) complex with $CoCp^*_2$, and an unstable Mo complex (**A**) was successfully observed at low temperature of 198 K. The EXAFS data clearly revealed that a part of the iodide ligands of **2** were removed from the Mo center and a structure coordinated with one iodide ligand was proposed based on the curve fitting analysis. Besides, XANES simulation suggested the six-coordination structure in the Mo center. From these insights, we proposed that **4** or **5** is formed under the reduction process of **2** at 198 K. **4** or **5** would be converted to **3** via **1** in the nitrogen atmosphere according to **eq. 1**.The observed complex of **4** or **5** that dinitrogen-bridged dimolybdenum complex **1** plays an important role as a key reactive intermediate for the scission of the bridging dinitrogen ligand in the Mo–N≡N–Mo core.[7i] Although further investigation is necessary to reveal the dinitrogen-bridged dimolybdenum structure, the insight obtained in this work leads to development in the discussion of the cleavage of the stable N≡N bond in dinitrogen by the Mo complexes. Besides, we believe that our investigation demonstrates the effectiveness of the methodology using DXAFS and simulation method for the characterization of the unstable key complex in the catalytic reaction.

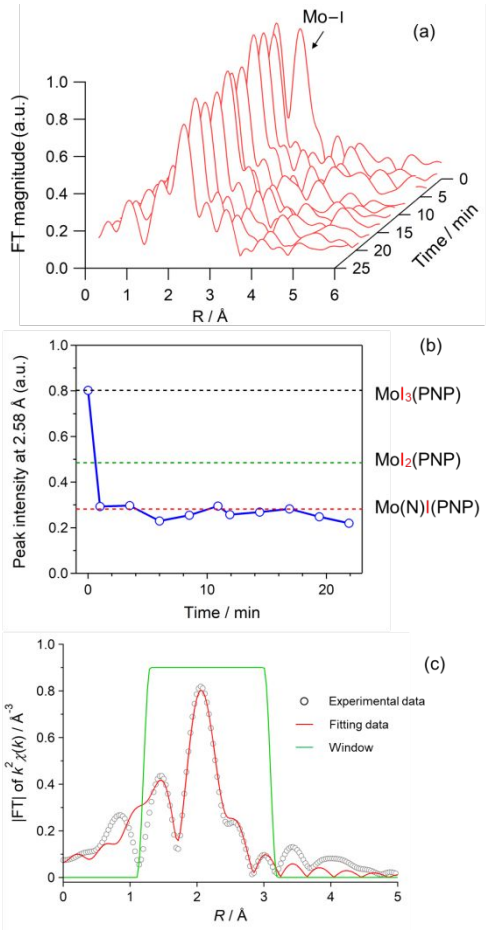

Fig. 3 (a) In situ Fourier-transformed EXAFS spectra before and after addition of $CoCp^*_2$ at 198 K. (b) Time-profile of the peak intensity at 2.58 Å. Dashed lines show the intensity at 2.58 Å in the reference samples. (c) The curve-fitting result of **A** (spectrum after 1 min from the addition of $CoCp^*_2$). The light green line shows the fitting window. Analysis condition: *k* weight: 2, *k* range: 3.0–10.9 $Å^{-1}$, *r* range: 1.2–3.1 Å.

Table 1. Curve-fitting result of the spectrum of **A** [a]

Shell	C.N. [b]	r [c] / Å	σ^2 [d]	ΔE [e]	R [f] (%)
Mo–N	3 [g]	2.00	0.0105	-9.5	
Mo–P	2 [g]	2.49	0.0011	6.8	1.4
Mo–I	1 [g]	2.74	0.0081	-13.8	

[a] Athena and Arthemis software were used for the analysis. Analysis condition: k weight: 2, k range: 3.0–10.9 Å^{-1}, r range: 1.2–3.1 Å. [b] Coordination number. [c] Bond distance. [d] Debye–Waller factor. [e] Edge shift. [f] R factor. [g] These values were fixed in the curve-fitting analysis.

Conflicts of interest

There are no conflicts to declare.

Acknowledgement

The present project is supported by CREST, JST (JPMJCR1541). The synchrotron radiation experiments were performed at the BL28B2 (2017A1511, 2017B1337) and BL01B1 (2017A1477) of SPring-8 with the approval of the Japan Synchrotron Radiation Research Institute (JASRI). This work was also performed under the approval of the Photon Factory Program Advisory Committee (2016G643). This work was supported by KAKENHI Grant number JP17H03117 (K.Y.), JP18K05148 (H.T.), 19K15359 (A.Y.), JP17H01201 (Y.N.), JP15H05798 (Y.N.), and JP18K19093 (Y.N.) from Japan Society for the Promotion of Science (JSPS) and the Ministry of Education, Culture, Sports, Science and Technology of Japan (MEXT).

Notes and references

1. (a) J. R. Jennings, *Catalytic Ammonia Synthesis*, Springer, Boston, MA, 1991. (b) H. Liu, *Ammonia synthesis catalysts : innovation and practice*, Chemical Industry Press and World Scientific: Singapore and Beijing, 2013.
2. D. V. Yandulov, R. R. Schrock, *Science*, 2003, **301**, 76.
3. For the selected review on nitrogen fixations catalysed by transition metal-dinitrogen complexes, see: (a) K. C. MacLeod, P. L. Holland, *Nat. Chem*, 2013, **5**, 559. (b) C. J. M. van der Ham, M. T. M. Koper, D. G. H. Hetterscheid, *Chem. Soc. Rev.*, 2014, **43**, 5183. (c) H.-P. Jia, E. A. Quadrelli, *Chem. Soc. Rev.*, 2014, **43**, 547. (d) C. Sivasankar, S. Baskaran, M. Tamizmani, K. Ramakrishna, *J. Organomet. Chem.*, 2014, **752**, 44. (e) D. R. Tyler, *Z. Anorg. Allg. Chem.*, 2015, **641**, 31. (f) N. Khoenkhoen, B. de Bruin, J. N. H. Reek, W. I. Dzik, *Eur. J. Inorg. Chem.*, 2015, 567. (g) R. J. Burford, M. D. Fryzuk, *Nat. Rev. Chem.*, 2017, **1**. (h) S. L. Foster, S. I. P. Bakovic, R. D. Duda, S. Maheshwari, R. D. Milton, S. D. Minteer, M. J. Janik, J. N. Renner, L. F. Greenlee, *Nat. Catal.*, 2018, **1**, 490. (i) N. Stucke, B. M. Floeser, T. Weyrich, F. Tuczek, *Eur. J. Inorg. Chem.*, 2018, 1337. (j) Y. Nishibayashi, *Dalton Trans.*, 2018, **47**, 11290. (k) Y. Nishibayashi, *Transition Metal-Dinitrogen Complexes: Preparation and Reactivity*, WileVCH: Weinheim, Germany, 2019. (l) Y. Tanabe, Y. Nishibayashi, *Coord. Chem. Rev.*, 2019, **389**, 73.
4. (a) R. R. Schrock, *Acc. Chem. Res.*, 2005, **38**, 955. (b) R. R. Schrock, *Angew. Chem. Int. Ed.*, 2008, **47**, 5512. (c) L. A. Wickramasinghe, T. Ogawa, R. R. Schrock, P. Mueller, *J. Am. Chem. Soc.*, 2017, **139**, 9132.
5. (a) J. S. Anderson, J. Rittle, J. C. Peters, *Nature*, 2013, **501**, 84–87. (b) T. J. Del Castillo, N. B. Thompson, D. L. M. Suess, G. Ung, J. C. Peters, *Inorg. Chem.*, 2015, **54**, 9256. (c) T. M. Buscagan, P. H. Oyala, J. C. Peters, *Angew. Chem. Int. Ed.*, 2017, **56**, 6921. (d) J. Fajardo, Jr., J. C. Peters, *J. Am. Chem. Soc.*, 2017, **139**, 16105. (e) M. J. Chalkley, T. J. Del Castillo, B. D. Matson, J. P. Roddy, J. C. Peters, *ACS Cent. Sci.*, 2017, **3**, 217. (f) M. J. Chalkley, T. J. Del Castillo, B. D. Matson, J. C. Peters, *J. Am. Chem. Soc.*, 2018, **140**, 6122.
6. L. R. Doyle, A. J. Wooles, L. C. Jenkins, F. Tuna, E. J. L. McInnes, S. T. Liddle, *Angew. Chem. Int. Ed.*, 2018, **57**, 6314.
7. (a) K. Arashiba, Y. Miyake, Y. Nishibayashi, *Nat Chem*, 2011, **3**, 120. (b) S. Kuriyama, K. Arashiba, K. Nakajima, H. Tanaka, N. Kamaru, K. Yoshizawa, Y. Nishibayashi, *J. Am. Chem. Soc.*, 2014, **136**, 9719. (c) H. Tanaka, K. Arashiba, S. Kuriyama, A. Sasada, K. Nakajima, K. Yoshizawa, Y. Nishibayashi, *Nat. Commun.*, 2014, **5**. (d) S. Kuriyama, K. Arashiba, K. Nakajima, H. Tanaka, K. Yoshizawa, Y. Nishibayashi, *Chem. Sci.*, 2015, **6**, 3940. (e) K. Arashiba, E. Kinoshita, S. Kuriyama, A. Eizawa, K. Nakajima, H. Tanaka, K. Yoshizawa, Y. Nishibayashi, *J. Am. Chem. Soc.*, 2015, **137**, 5666. (f) S. Kuriyama, K. Arashiba, K. Nakajima, Y. Matsuo, H. Tanaka, K. Ishii, K. Yoshizawa, Y. Nishibayashi, *Nat. Commun.*, 2016, **7**. (g) S. Kuriyama, K. Arashiba, H. Tanaka, Y. Matsuo, K. Nakajima, K. Yoshizawa, Y. Nishibayashi, *Angew. Chem. Int. Ed.*, 2016, **55**, 14289. (h) A. Eizawa, K. Arashiba, H. Tanaka, S. Kuriyama, Y. Matsuo, K. Nakajima, K. Yoshizawa, Y. Nishibayashi, *Nat. Commun.*, 2017, **8**. (i) K. Arashiba, A. Eizawa, H. Tanaka, K. Nakajima, K. Yoshizawa, Y. Nishibayashi, *Bull. Chem. Soc. Jpn.*, 2017, **90**, 1111. (j) Y. Sekiguchi, K. Arashiba, H. Tanaka, A. Eizawa, K. Nakajima, K. Yoshizawa, Y. Nishibayashi, *Angew. Chem. Int. Ed.*, 2018, **57**, 9064. (k) T. Itabashi, I. Mori, K. Arashiba, A. Eizawa, K. Nakajima, Y. Nishibayashi, *Dalton Trans.*, 2019, **48**, 3182. (l) A. Eizawa, K. Arashiba, A. Egi, H. Tanaka, K. Nakajima, K. Yoshizawa, Y. Nishibayashi, *Chem. Asian J.*, 2019, **14**, 2091. (m) Y. Ashida, K. Arashiba, K. Nakajima, Y. Nishibayashi, *Nature*, 2019, **568**, 536. (n) Y. Ashida, K. Arashiba, H. Tanaka, A. Egi, K. Nakajima, K. Yoshizawa, Y. Nishibayashi, *Inorg. Chem.*, 2019, **58**, 8927. (o) Y. Ashida, S. Kondo, K. Arashiba, T. Kikuchi, K. Nakajima, S. Kakimoto, Y. Nishibayashi, *Synthesis*, 2019, **51**, 3792.
8. For example, see: (a) Y. Chen, J. L. Fulton, J. C. Linehan, T. Autrey, *J. Am. Chem. Soc.*, 2005, **127**, 3254. (b) J. L. Fulton, J. C. Linehan, T. Autrey, M. Balasubramanian, Y. Chen, N. K. Szymczak, *J. Am. Chem. Soc.*, 2007, **129**, 11936. (c) A. S. K. Hashmi, C. Lothschütz, M. Ackermann, R. Doepp, S. Anantharaman, B. Marchetti, H. Bertagnolli, F. Rominger, *Chem. Eur. J.*, 2010, **16**, 8012. (d) M. Bauer, C. Gastl, *Phys. Chem. Chem. Phys.*, 2010, **12**, 5575. (e) C. Garino, E. Borfecchia, R. Gobetto, J. A. van Bokhoven, C. Lamberti, *Coord. Chem. Rev.*, 2014, **277-278**, 130. (f) H. Takaya, S. Nakajima, N. Nakagawa, K. Isozaki, T. Iwamoto, R. Imayoshi, N. J. Gower, L. Adak, T. Hatakeyama, T. Honma, M. Takagaki, Y. Sunada, H. Nagashima, D. Hashizume, O. Takahashi, M. Nakamura, *Bull. Chem. Soc. Jpn.*, 2015, **88**, 410. (g) Agata, H. Takaya, H. Matsuda, N. Nakatani, K. Takeuchi, T. Iwamoto, T. Hatakeyama, M. Nakamura, *Bull. Chem. Soc. Jpn.*, 2018, **92**, 381. (h) N. B. Thompson, M. T. Green, J. C. Peters, *J. Am. Chem. Soc.*, 2017, **139**, 15312. (i) K. Nomura, G. Nagai, I. Izawa, T. Mitsudome, M. Tamm, S. Yamazoe, *ACS Omega*, 2019, **4**, 18833.
9. B. Ravel, M. Newville, *J. Synchrotron Rad.*, 2005, **12**, 537.
10. O. Bunău, Y. Joly, *J. Phys.: Condens. Matter*, 2009, **21**, 345501.
11. No difference was observed in the simulation results using the structures of three isomers. See, **Fig. S4**.
12. R. G. Leliveld, A. J. van Dillen, J. W. Geus, D. C. Koningsberger, *J. Catal.*, 1997, **165**, 184.
13. (a) T. E. Westre, P. Kennepohl, J. G. DeWitt, B. Hedman, K. O. Hodgson, E. I. Solomon, *J. Am. Chem. Soc.*, 1997, **119**, 6297. (b) T. Yamamoto, *X-Ray Spectrom.*, 2008, **37**, 572−584.
14. We carried out the curve-fitting analysis of Fourier-transformed EXAFS spectra of **2**, and confirmed the band at a radial distance of 2.58 Å is mainly composed by the Mo-I scattering. For the details, see **Fig. S5** and **Table S3** in **ESI**.
15. We measured the two dimolybdenum complexes of $[MoCl_2(\mathbf{PNP})]_2(\mu\text{-}N_2)$ and $[Mo(N_2)_2(\mathbf{PNP})]_2(\mu\text{-}N_2)$ using a conventional XAFS (Quick-XAFS) tequnique in NW10A (KEK-PF, Japan) at room temperature (**ESI**). In $[MoCl_2(PNP)]_2(\mu\text{-}N_2)$/THF, we confirmed the small Mo-Mo band around 4.7 Å. However, in $[Mo(N_2)_2(PNP)]_2(\mu\text{-}N_2)$/THF, the Mo-Mo band was not found clearly (**Fig. S6**). Thus, it is difficult to determine whether **4** or **5** is the formed Mo complex (**A**) only based on the DXAFS data.

Table of Contents (maximum size 8 cm x 4 cm)

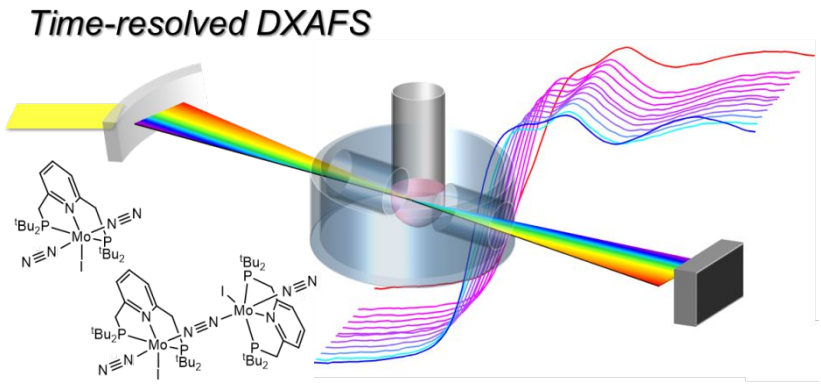

Dispersive XAFS (DXAFS) was used for the structural characterization of a hardly-isolatable molybdenum-dinitrogen complex bearing a PNP-type pincer ligand.